



# Determination of Fatigue Life of Surface Propeller by Using Finite Element Analysis

R. Surendra Rao<sup>1</sup>, Shuvendra Mohan<sup>2</sup>, G. Sawan Kumar<sup>3</sup>

Mechanical Engineering Department, Kasi reddy naryan reddy college of engineering and research, Hyderabad, India<sup>1</sup>

Aeronautical Engineering Department, Institute of Aeronautical Engineering, Hyderabad, India<sup>2</sup>

Aeronautical Engineering Department, Kasi reddy naryan reddy college of engineering and research, Hyderabad, India<sup>3</sup>

## Abstract:

Propeller design aims at achieving high propulsive efficiency at low levels of vibration and noise, usually with minimum cavitations. Achieving this aim is difficult with conventional propellers, as ships have become larger and faster propeller diameters have remained limited by draught and other factors. Surface piercing propeller offers an attractive alternative to high-speed crafts, which operate under limited draught. The performance of the vehicle depends upon the efficiency of the propeller. The geometric shape and its surface finish will decide the efficiency of the propeller. The material used is carbon UD and aluminum. The present project basically deals with the modeling, Analysis of the propeller using composite material of a marine vehicle having low draft. A propeller is complex 3D model geometry. CATIA modeling software is used for generating the blade model and tool path on the computer. Sectional data, pitch angle of the propeller are the inputs for the development of propeller model. Finite element analysis was carried out using ABAQUS. The propeller model developed in CATIA is converted in to IGES file and then imported to HYPERMESH for developing fine mesh of the model. As a part of the analysis static structural testing was conducted by varying material properties in pre-processing stage. Further fatigue analysis was performed to analyze the factor of safety. Based on the results obtained from both static analysis and dynamic analysis a better performing material is identified for the development of a propeller. The post processed results obtained from both analysis methods recommends carbon UD/ Epoxy for the fabrication of propeller.

**Keywords:** Abaqus, Blade Angle, Catia, Hyper Mesh Pitch angle, Propeller Blades Surface piercing

## I. INTRODUCTION

A propeller is a type of fan that transmits power by converting rotational motion into thrust. A pressure difference is produced between the forward and rear surfaces of the airfoil-shaped blade, and air or water is accelerated behind the blade. Propeller dynamics can be modeled by both Bernoulli's principle and law. A propeller is the most common propulsion on ships, imparting momentum to a fluid which causes a force to act on the ship. Three, four, or five blades are most common in marine propellers, although designs which are intended to operate at reduced noise will have more blades. The blades are attached to a boss (hub), which should be as small as the needs of strength allow - with fixed pitch propellers the blades and boss are usually a single casting.

A ship needs propulsion system to move in water, so by using a thrust – producing mechanism the ship moves. There are many thrust-producing devices called propellers like screw propellers, pump jet, water jet etc which producing by high speed crafts, ships, pleasure crafts and torpedoes. The speed of marine vehicle depends on the choice of propulsion system. The thrust from the propeller is transmitted to move the ship through a transmission system which consists of a rotational motion generated by the main engine crank shaft, intermediate shaft and its bearings, stern tube shaft and its bearing and finally by the propeller itself.

Surface piercing propeller has emerged as an integrated solution for high-speed craft, to overcome the problems such as cavitations, low draught & shallow water restrictions that is prominent with these crafts. It is also easily adaptable for different operating speeds. These propellers operate in partially submerged condition, mostly in inclined position and draws in air bubble along the blade on the back surface. The air bubbles contract or expand on the surface all along its

underwater operation and avoid cavitations and its implied problems like vibration, erosion and thrust breakdown. This propeller eliminates the appendage drag due to the brackets, shafts including the drag due to Magnus effect of the rotating shaft. In is best suitable for small and high-speed crafts and has virtually no limit on size of propeller due to draught restrictions. These propellers are freely adoptable for large range of vehicle speeds by adjusting the immersion. It is suitable for very high craft to attain high speeds. Steering requirements also can be met partially by adjustment of the angles of the shaft.

## II. LITERATURE REVIEW

Surface Piercing Propellers (SPP) are marine semi-submerged propellers used for high speed crafts. These propellers operate at the surface of the water for a superior performance, and thus they are subjected to severe hydrodynamic pressures. SPPs are commonly made of stainless steel materials. Designing a novel composite SPP is the basic purpose of the investigation carried out by M. S. Kiasat, L. Babae, Department of Marine Tech., Amirkabir University of Technology. The mechanical loads considered in this work are the hydrodynamic pressure, the centrifugal force and the gravity. The non-uniform distribution of the hydrodynamic pressure on the surface of the blades is obtained through a boundary element analysis in another related work. A stainless steel propeller modeled by using solid tetrahedral finite elements is analyzed and compared to a composite propeller modeled by using quadrilateral shell elements. The composite blades consist of a carbon/epoxy laminated skin and a less stiff core. Large strain nonlinear progressive failure analyses are carried out. The results show that the maximum stresses occur along the leading and the trailing edges of the blade.

The steel propeller begins to fail on its edges at 90% of the maximum hydrodynamic pressure, while the designed carbon/epoxy composite propeller can safely carry the full loading. Further, the buckling of the composite blade under the hydrodynamic pressure is observed.

Work carried out by Dr. y. seetharamarao Dept of Mechanical Engg., G.V.P. College Of Engineering, Visakhapatnam, proposes a methodology to design a propeller with a metal and composite material to analyze its strength and deformation using Ansys software. In order to evaluate the effectiveness of composite over metals, stress analysis is performed on both composite and metal propeller using Ansys. Proposed methodology showed substantial improvements in metal propellers. The mean deflection, normal stress and shear stress were found for both metallic and composite propeller by using Ansys. From the results, stress analysis composite propeller is safe resonance phenomenon. In this work effort is made to reduce stress levels so that advantage of weight reduction along with stresses can be obtained. The comparison analysis of metallic and composite propeller was made for the maximum deformation and normal stresses.

Since most past methods assumed the blades to be perfectly rigid, the structural response can be computed separately by applying the blade pressure obtained from the hydrodynamic model. The most extensively used structural model is based on the modified cantilever beam theory developed by Taylor (1933). It assumed the blade to be a cantilever beam loaded by thrust and torque distributed linearly over the radius (Schoenherr, 1963). Later, modifications were made to include the effects of rake, skew, and centrifugal force (Morgan, 1954; Schoenherr, 1963; Atkinson, 1968). The beam theory has been shown to be suitable for estimating the stress near the roots of propeller blade with conventional geometry and relatively narrow plan form. However, it cannot accurately predict stress distribution for complex blade geometries (e.g. propellers with high skew, wide blade outline, or vastly asymmetrical blade sections). To improve blade stress predictions, a thin-shell approach was introduced by Conolly (1961). However, due to the assumption of symmetrical forms and normal deflections, this approach was appropriate only for wide blade geometries. To overcome the limitations of shell theory, finite element methods (FEMs) have been employed for blade strength analysis since the

early 1970's. Notable studies in this area include the works of Genalis (1970) using triangular plane elements, Sontvedt (1974) using thin-shell elements, Atkinson (1973) using super-parametric thick shell elements, and Ma (1974) using 3-D quadratic isoparametric brick elements. In all of these models, the fluid pressure acting on the blade surface was obtained by employing either the quasi-steady method, lifting line method, or lifting surface method. The effects of fluid-structure interactions were ignored, i.e. the fluid pressure were determined using the undeformed blade geometry. The results indicated that the FEM is more accurate than the other methods for predicting steady and unsteady blade stresses, particularly for extreme propeller geometries.

To account for change in fluid pressure due to blade deformation, an iterative procedure was developed by Atkinson and Glover (1988). A lifting surface method was used to determine the fluid pressure, which was imposed on the blade surface to obtain the change in blade geometry via a FEM, and the process was repeated until a stable operating condition was reached. The effect of cavitation was considered, but the study was limited to steady flow conditions (Atkinson and Glover, 1988). Thus, the dynamic blade stress and the effect of fluid-structure interaction on the

hydrodynamic performance cannot be captured. Later, a coupled approach was introduced by Kuo and Vorus (1985) for dynamic blade stress analysis. A potential-based method was used to determine the hydrodynamic blade load, as well as the added mass and damping associated with elastic blade motion due to unsteady pressure loading. The coupled problem was solved in the frequency domain using a FEM with 3-D linear iso-parametric brick elements (Kuo and Vorus, 1985). Nevertheless, the method was limited to the dynamic analysis of non cavitating fully submerged propellers, and the effect of blade displacement on the fluid pressure was ignored (i.e. the change in influence coefficients due to blade deformation were assumed to be negligible). A nonlinear coupled strategy for hydro elastic blade analysis using the FEM and lifting surface methods was also developed by Lin and Lin (1996). The change in influence coefficients due to blade displacement was included, and the effect of geometric nonlinearity was considered. However, the work was limited to steady, non cavitating propellers. Thus, the dynamic blade loads and stress distributions cannot be obtained.

Surface piercing propellers were first patented by David Napier in 1841. Later on few experimental studies of surface piercing propellers were made but their application was not pronounced. Wang, and Nozawa and Takayama published their experimental investigations and testing methodologies in 1990s. Dyson also conducted series of experiments to determine the dynamic performance of partially submerged propellers.

Moreover, few numbers of analytical methods in this field have been conducted. The first known method for the analysis of surface piercing propellers was developed by Yegorov and Sadovnikov. They applied a blade element method based on two-dimensional hydrofoil theory, but ignored the effect of adjacent blades, cavities, and wake vortex sheets. Kudo and Ukon developed a three dimensional lifting surface vortex lattice method for the analysis of super cavitating propellers which has been extended for the analysis of surface piercing propellers.

A 3-D potential-based boundary element method (BEM) is coupled with a 3-D finite element method (FEM) for the time-dependent hydro elastic analysis of cavitating propulsors. The BEM is applied to evaluate the moving cavity boundaries and fluctuating pressures, as well as the added mass and hydrodynamic damping matrices. The FEM is applied to analyze the dynamic blade deformations and stresses due to pressure fluctuations and centrifugal forces. The added mass and hydrodynamic damping matrices are superimposed onto the structural mass and damping matrices, respectively, to account for the effect of fluid-structure interaction. The problem is solved in the time-domain using an implicit time integration scheme. An overview of the formulation for both the BEM and FEM is presented, as well as the BEM/FEM coupling algorithm. The effects of fluid-structure interaction on the propeller performance are discussed by Y.L. Young<sup>Ã</sup>, Department of Civil and Environmental Engineering, Princeton University.

This paper treats the unsteady cavitating turbulent flow around a full scale marine propeller operated in non-uniform ship wake. The RANS method combined with  $k-\omega$  SST turbulence model and the mass transfer cavitation model was applied for the flow simulation. It is noted that both the propeller performance and the unsteady features of cavitating turbulent flow around the propeller predicted by the numerical calculation agreed well with the experimental data. Due to the non-uniform wake inflow and gravity effect, there

occurred periodical procedure for cavity development such as cavitation inception, growth, shrinking, etc near the blade tip for the propeller. The study also indicated that there was consider a blylarge pressure fluctuation near the propeller during the operation. The 1st order frequency of pressure fluctuation predicted by numerical simulation equaled the rotating frequency of propeller blades. Both amplitude and frequency agreed with the experimental results fairly well.

Lin developed an early numerical model for the 3-D analysis of a composite marine propeller. He compared the stress evaluations for the composite propeller and a geometrically identical metal propeller. The composite blade was constructed of a laminated thick-shell skin over a foam core. Lin and Lin presented a coupled 3-D FEM/VLM method for the hydro elastic analysis and strength evaluation of composite marine propellers. The effect of geometric nonlinearities was considered. Most recently, Young et al. presented several works on the hydro elastic and time dependent analysis of marine composite propellers. An overview of the developments in the composite propeller industries was presented by Marsh. A few companies have realized the potential and claimed to have designed composite marine propellers with passive properties. Nonetheless, no details of those developments have yet been published.

The work focuses on the structural analysis and design of a novel composite surface piercing propeller. The mechanical loads to be applied to the propeller are the hydrodynamic pressure, the centrifugal force and the gravity. The non-uniform distribution of the hydrodynamic pressure on the surface of the blades is obtained through a boundary element analysis in another related work. A stainless steel propeller modeled by using solid finite elements is analyzed and compared to a composite propeller modeled by using shell elements. The composite blades consist of a carbon/epoxy laminated skin and a less stiff core. Large strain nonlinear progressive failure analyses using various failure criteria are carried out taking the stiffness degradation process into account.

The use of an unsteady computational fluid dynamic analysis of the manoeuvring performance of a self-propelled ship carried out by Alexander B. Phillips a, Stephen R, School of Engineering Sciences, University of Southampton, requires a large computational resource that restricts its use as part of a ship design process. A method is presented that significantly reduces computational cost by coupling a blade element momentum theory (BEMT) propeller model with the solution of the Reynolds Averaged Navier-Stokes (RANS) equations. The approach allows the determination of maneuvering coefficients for a self-propelled ship travelling straight ahead, at a drift angle and for differing rudder angles. The swept volume of the propeller is divided into discrete annuli for which the axial and tangential momentum changes of the fluid passing through the propeller are balanced with the blade element performance of each propeller section. Such an approach allows the interaction effects between hull, propeller and rudder to be captured. Results are presented for the fully appended model scale self-propelled KRISO very large crude carrier 2 (KVLCC2) hull form undergoing static rudder and static drift tests at a Reynolds number of  $4.6 \times 10^6$  acting at the ship self-propulsion point. All computations were carried out on a typical workstation using a hybrid finite volume mesh size of  $2.1 \times 10^6$  elements. The computational uncertainty is typically 2–3% for side force and yaw moment.

Surface-Piercing Propellers (SPPs) are the preferred propulsion system for light to moderately loaded high-speed applications due to the high fuel efficiency. For highly loaded

applications, the efficiency of SPPs tends to decrease because of the limited submerged blade area and the presence of large suction side cavities. Moreover, it is a challenge to design large-scale SPPs that can maintain reliable fatigue strength and avoid vibration issues while maximizing the propeller thrust for a given power input.

Work By Yin Lu Young a, Brant R. Savanderb Department of Naval Architecture and Marine Engineering, University of Michigan, Ann Arbor, three SPP designs are presented for different size Surface Effect Ships (SEs) that can attain maximum advance speed of 25.72 m/s (50 knots). A previously developed and validated three-dimensional (3-D) coupled boundary element method–finite element method (BEM–FEM) is used for the transient hydro elastic analysis of SPPs. The method is validated by comparing the predicted hydrodynamic performance with those obtained using a vortex-lattice method (VLM) and a Reynolds Averaged Navier–Stokes (RANS) solver. The hydrodynamic and structural dynamic performance of the SPPs are presented. Finally, challenges associated with the design related analyzes of large-scale SPPs are discussed.

The application of composite technology to marine applications has with particular benefits of its lightweight, less noise, pressure fluctuations and fuel consumption [1]. The finite element method is so popular and has been used many researchers [2]. The research and development of propellers using composites are advancing. The back drop to this advancement is the fact that composites can provide a wide variety of special characteristics that metals can not. In terms of cost, as well as diffusion rates of composites is rapid, technology advances yearly and the costs of composites are becoming cheaper [3]. More over composites can offer the potential benefits corrosion resistance and fatigue performance, improved material damping properties and reduced life time maintenance cost [4]. Taylor [5] considered a propeller blade as a cantilever rigid at the boss. J.E Conolly [6] combined theory and with experimental work for wide blades. Chang suplee [7] investigated the main sources of propeller blade failure and resolved the problems related to blades symmetrically. G.H.M Beet[8] examined the interference between the stress conditions in the propeller blade and the hub. W.J.Colcough [9] studied the advantages of a composite propeller blade with fibre reinforced plastic over that of the propeller blade made from over materials. GauFengLin [10] carried out a stress calculations for fiber reinforced composite thrust blade.

### III. PROPELLER MATERIALS

#### A. Materials:

The material used for propellers must be light, strong and ductile, easy to cast and machine, and resistant to erosion and corrosion. The Ship propeller may be manufactured from commercially available material like gray cast iron, carbon and low-alloy steels, nickel-manganese bronze, nickel-aluminum bronze, Naval brass, forged aluminum, composite materials etc.

#### A.1 Types of Composite Materials:

Composite materials are as follows

- Glass fibre
- Aramid fibre
- Carbon fibre (Standard Grade )
- Carbon fibre (Special Grade)
- Glass-reinforced plastic (GRP)
- Carbon UD/EPOXY

#### Carbon UD/Epoxy:

Carbon fiber reinforced polymer carbon reinforced plastic (CFRP or CRP), is a very strong, light, and

expensive composite material or fiber-reinforced polymer. Similar to fiberglass (glass reinforced polymer), the composite material is commonly referred to by the name of its reinforcing fibers (carbon fiber). The polymer is most often epoxy, but other polymers, such as polyester, vinyl ester or nylon, are sometimes used. Some composites contain both carbon fiber and other fibers such as Kevlar, aluminum, and fiberglass reinforcement. The terms graphite-reinforced polymer or graphite fiber-reinforced polymer (GFRP) are also used, but less commonly, since glass-(fiber)-reinforced polymer can also be called GFRP. In product advertisements, it is sometimes referred to simply as graphite fiber (or graphite fiber), for short.

It has many applications in aerospace and automotive fields, as well as in sailboats, and notably in modern bicycles and motorcycles, where its high strength-to-weight ratio is of importance. Improved manufacturing techniques are reducing the costs and time to manufacture, making it increasingly common in small consumer goods as well, such as lap tops, tripods, fishing rods, paint ball equipment, archery equipment, racquet frames, bodies, classical strings, drum shells, golf clubs, and pool/billiards/snooker cues.

TABLE: 1  
PROPERTIES OF CARBON UD/EPOXY MATERIAL

S.No	Young's Modulus variables	Young's Modulus values
1	$E_x$ (Gpa)	25
2	$E_y$ (Gpa)	10
3	$E_z$ (Gpa)	10
4	$\nu_{xy}$	0.16
5	$\nu_{yz}$	0.48
6	$\nu_{zx}$	0.16
7	$G_{xy}$ (Gpa)	5.2
8	$G_{yz}$ (Gpa)	3.8
9	$G_{zx}$ (Gpa)	6
10	Density $Ns^2/mm^4$	$1.6 \times 10^{-3}$

#### IV. PROPELLER MODELING USING CATIA

CATIA is used for modeling of propeller, it provides multiple surface and solids-based machining for a full range of parts, from 2-Axis work to complex 3-axis moulds, dies and prototypes.

##### A. Introduction to Propeller Geometry:

A propeller consists of a number of identical blades on a boss. The propeller is usually fitted at the aft end of the ship. The surface of a propeller blade, which faces aft is called its Face, the opposite surface being the Back of the blade. The junction of the blade to the boss is the blade root and the extremity of the blade (the point farthest from the center of the propeller) is the blade tip. The blades of a propeller; the sometimes inclined aft with respect to the axis of the rotating of the propeller; the propellers are then said to have rake. The inclination of the propeller blade in a plane normal to the propeller axis is called skew. When the propeller is rotating so as to cause the ship to move forward, the front edge (with respect to the motion) is called the leading edge of the propeller blade propeller blade, while the rear edge is called the trailing. The diameter of the circle traced out by the blade tips when the propeller is turning is called the propeller diameter (D).

CATIA allows for creation of complete three-dimensional models of parts. The part model can be used to (i) produce fully-dimensioned engineering drawings for manufacturing the part (ii) Generate the tool path (iii) Verify tool path (iv) Generate NC part program for NC machines (v) Generates inputs for analytical processes such as Finite

element analysis. These components are modeled by using the geometric entities like Points, Curves, surface, etc.

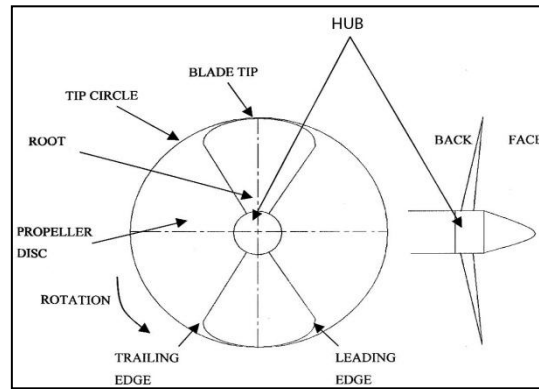


FIG: 1 GEOMETRY OF THE PROPELLER

##### B. Generating Propeller Geometry in CATIA:

The blade is divided into fourteen sections over the blade radius. Since the coordinate point data for the blade sections are more, the sections data is converted into a machine code language file.

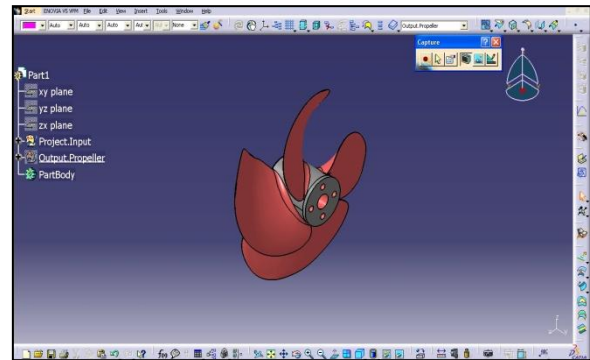


FIGURE:2 PROJECT INPUT

Follow the same path as discussed below for all the fourteen section.

- Start the CATIA and select new
- Select start and then Modeling
- Select sketch and select the XY plane
- Draw a circle with 50mm diameter and finish sketch
- Select the circle and Extrude (-50,50) and ok
- Select splines, through points, points from file and
- Select the splines and edit, transform and translate

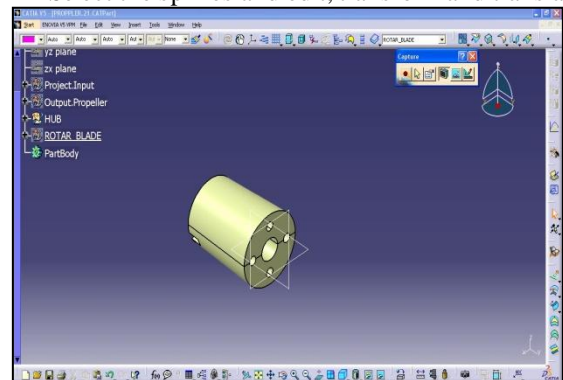


FIGURE: 3 HUB MODEL DEVELOPED IN CATIA

- Select delta and give XC value ,ok and move
- Rotate between two axes and select the YC and rotate 90
- Translate the splines in Y axis and give the value
- Rotate between two axes in X axis and give the value and ok
- Create a datum plane
- Wrap the splines into the circle.

- Join all the splines which forms the blade curvature and then ruled it.
- Using rotate option> select the blade and rotate it.

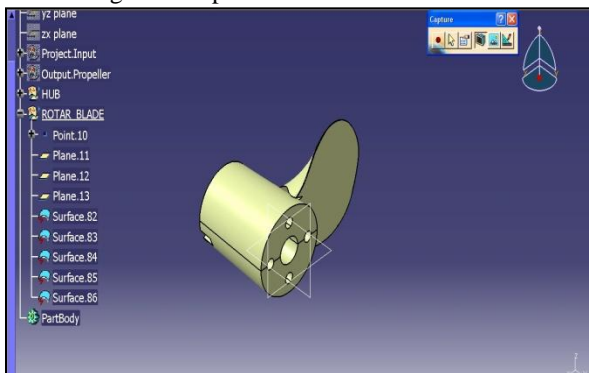


FIGURE: 4 ONE BLADE OF THE PROPELLER

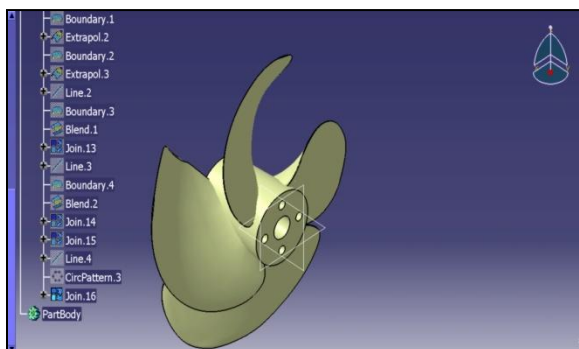


FIGURE: 5a MODEL OF SURFACE PIERCING PROPELLER DEVELOPED

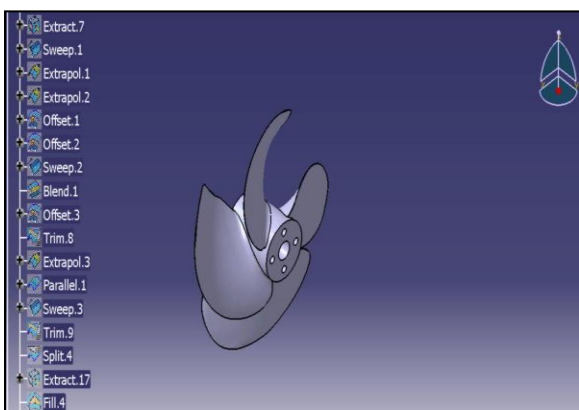


FIGURE: 5b MODEL OF SURFACE PIERCING PROPELLER DEVELOPED

## V. ANALYSIS OF PROPELLER USING ABAQUS

### A. MESH THE GEOMETRY (USING HYPER MESH) MESH SPECIFICATION:

Meshing is the procedure of applying a finite number of elements to the model. In order to conduct a finite element analysis the structure must be first idealized into some form of mesh. The art of successful application of the technique, so far as the user is concerned, lies in the combined choice of element types and associated mesh. As the method it approximates, it is necessary that the user have a good idea of the form of the solution, together with an understanding of the consequences of the assumptions made within the element types to be used.

### B. ELEMENT TYPE:

#### ELEMENT TYPE FOR STRUCTURAL ANALYSIS:

Picking an element type from the large library of elements in ABAQUS can be an intimidating thing for a

beginner. The following are the two types elements which are used for meshing.

- Hexa – C3D8
- Penta – C3D6
- Hexa C3d8/ Eight-Node Brick Element.

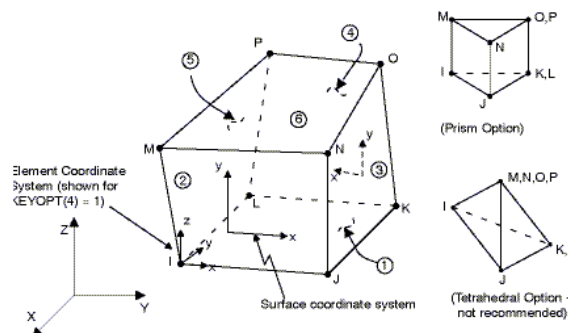


FIGURE: 6 HEXA C3D8GEOMETRY

### HEXA C3D8 INPUT SUMMARY:

Element Name	C3D8
Nodes	I, J, K, L, M, N, O, P
Degrees of Freedom	$U_x, U_y, U_z$
Real constants	None

Material Properties  $E_x, E_y, E_z, ALP_x, ALP_y, ALP_z,$

$PR_{xy}, PR_{yz}, PR_{xz}, DENS, G_{xy},$

$G_{yz}, G_{xz}, DAMP$

Surface Loads Pressures:  
face 1 (J-I-L-K), face 2 (I-J-N-M), face 3 (J-K-O-N),  
face 4 (K-L-P-O), face 5 (L-I-M-P), face 6 (M-N-O-P)

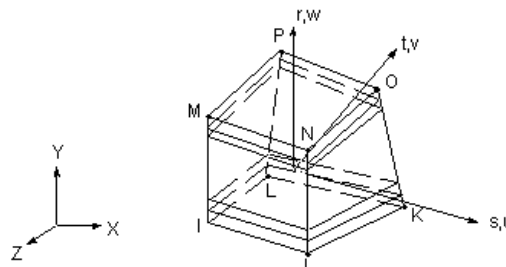


FIG: 7 HEXA - 3-D 8- NODE LAYERED STRUCTURAL SOLID ASSUMPTIONS AND RESTRICTIONS

All material orientations are assumed to be parallel to the reference plane, even if the element has nodes inferring warped layers. The numerical integration scheme for the thru-thickness effects are identical to that used in SHELL4 noded element. This may yield a slight numerical inaccuracy for elements having a significant change of size of layer area in the thru-thickness direction. The main reason for such discrepancy stems from the approximation of the variation of the determinant of the Jacobian in the thru-thickness direction. The error is usually insignificant

. However, users may want to try a patch-test problem to assess accuracy for their particular circumstances. Unlike shell elements, HEXA cannot assume a zero transverse shear stiffness at the top and bottom surfaces of the element. Hence the intern laminar shear stress must be computed without using this assumption, which leads to relatively constant values thru the element. The use of effective ("eff") material

properties developed below is based on heuristic arguments and numerical experiences rather than on a rigorous theoretical formulation. The fundamental difficulty is that multi linear displacement fields are attempted to be modeled by a linear (or perhaps quadratic) displacement shape function since the number of DOF per element must be kept to a minimum. A more rigorous solution can always be obtained by using more elements in the thru-the-layer direction. Numerical experimentation across a variety of problems indicates that the techniques used with HEXA give reasonable answers in most cases.

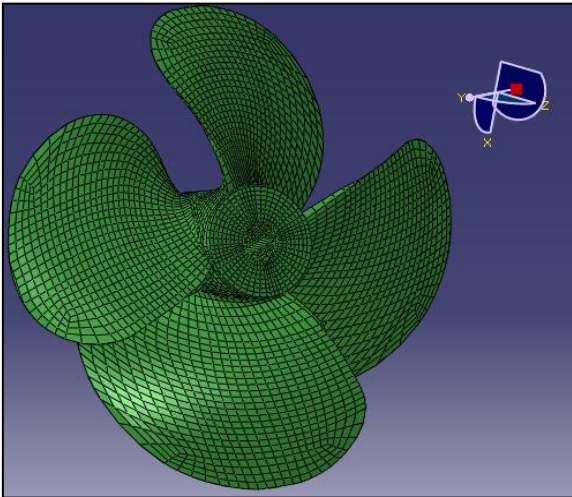


FIGURE: 8 FE MODEL OF PROPELLER

**C. IMPORTING FILE TO ABAQUS:**

The model created in CATIA is imported into ABAQUS using the IGES/IGS file.

By using the following procedure file can be imported:

- STEP I : Select file option and import using part format.
- STEP II : Browse the file from the selected location and open it.

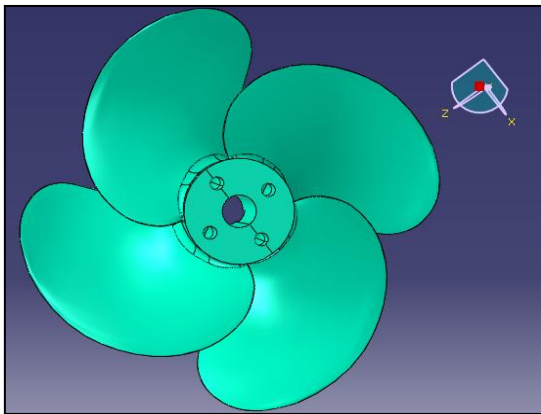


FIGURE:9 PROPELLER GEOMETRY IMPORTED TO ABAQUS

**D. MATERIAL PROPERTIES:**

Select the material module option and select material manager.

- After that we have to define the material properties.
- Select section manager and call material properties in this section.
- Assign the section by picking the part.

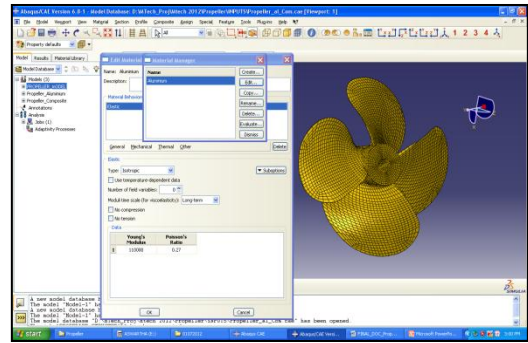


FIGURE:9 ASSIGNING THE MATERIAL PROPERTIES

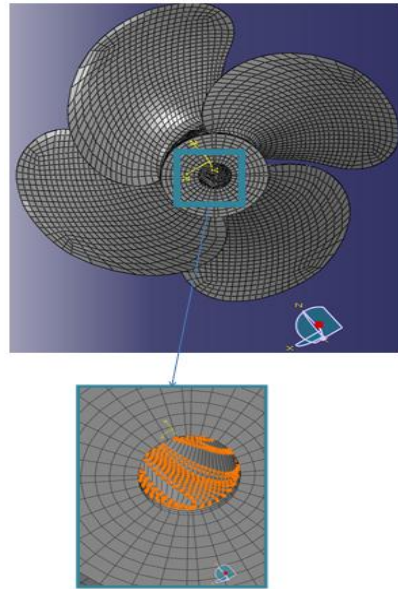


FIGURE: 10 BOUNDARY CONDITIONS APPLIED ON THE NODES

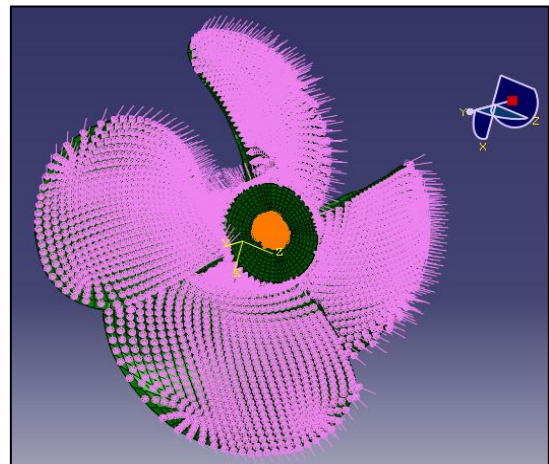


FIGURE: 11 PRESSURE LOADS APPLIED ON THE PROPELLER BLADES

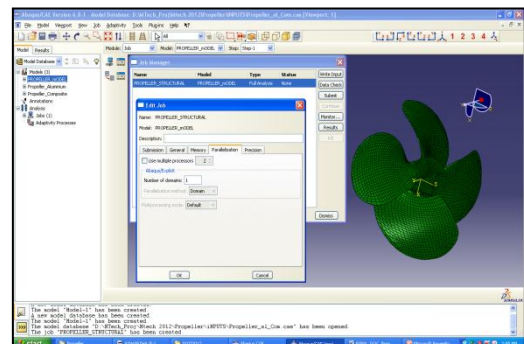


FIGURE: 12 SOLVING USING ABAQUS

## VI. RESULTS

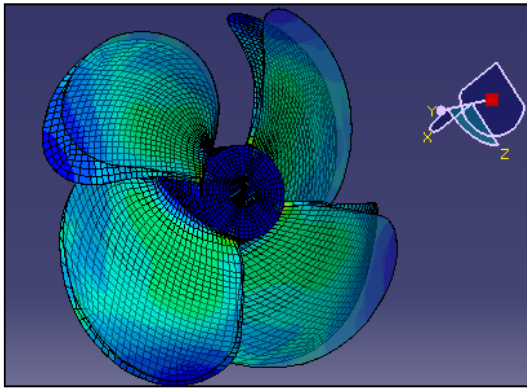


FIGURE: 13 DEFORMATION OF THE PROPELLER

### A. MATERIAL ALUMINUM

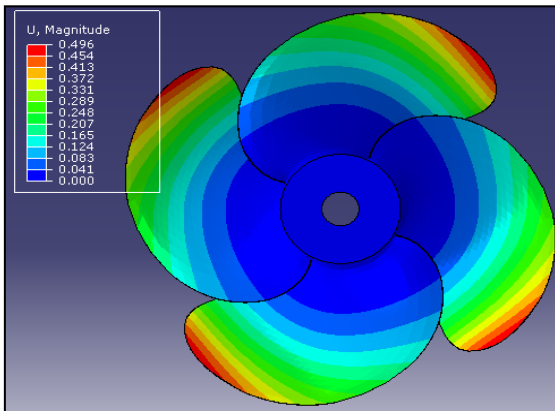


FIGURE: 14 DISPLACEMENT VECTOR SUM

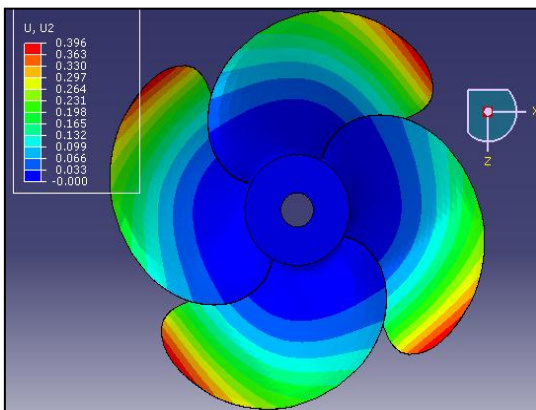


FIGURE: 15 DISPLACEMENT IN Y-DIRECTION

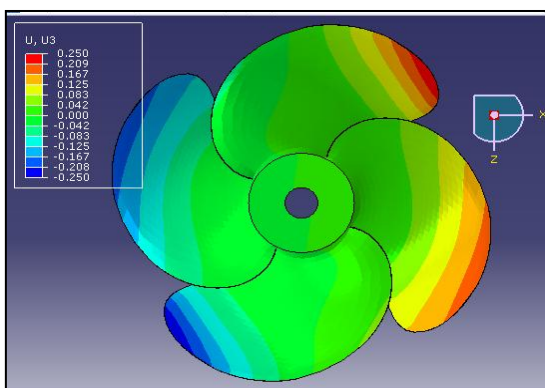


FIGURE: 16 DISPLACEMENT IN Z-DIRECTION

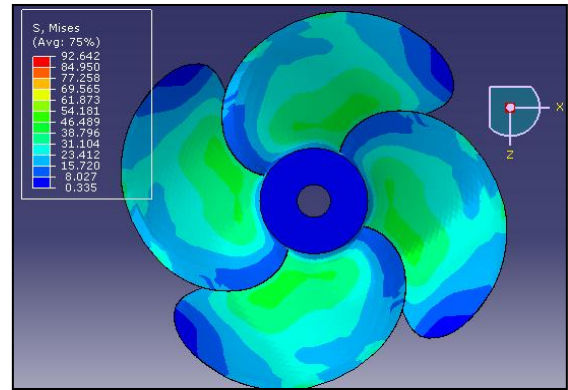


FIGURE: 17 VON MISES STRESS

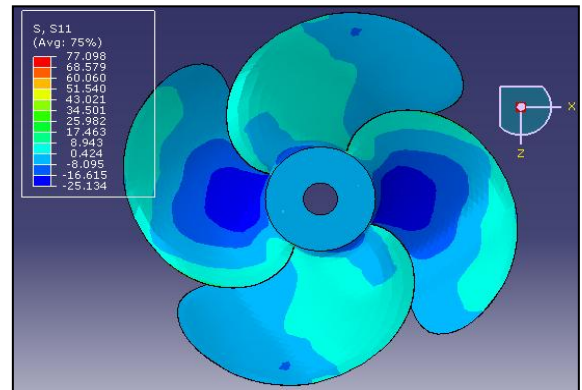


FIGURE: 18 STRESSES IN X- DIRECTION

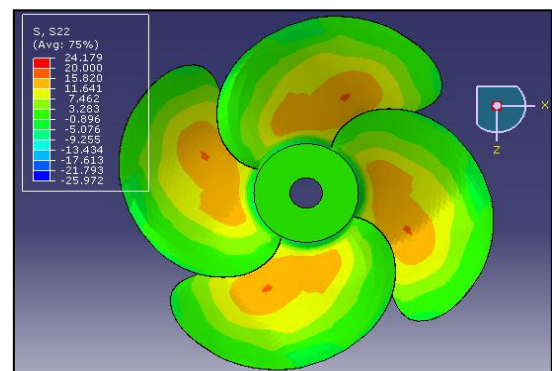


FIGURE: 19 STRESSES IN Y-DIRECTION

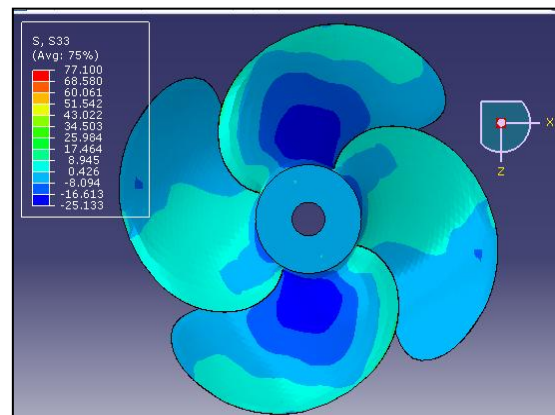


FIGURE: 20 STRESSES IN Z-DIRECTION

## B. COMPOSITE MATERIAL

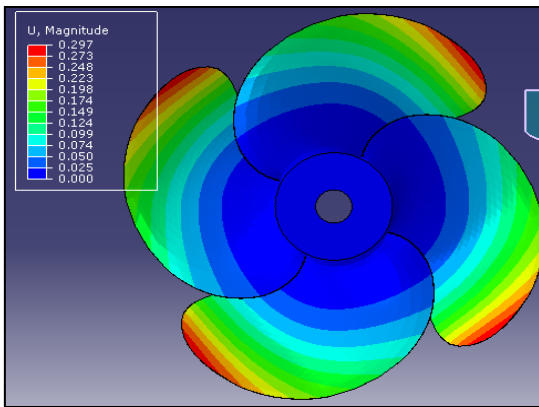


FIGURE: 21 DISPLACEMENT VECTOR SUM

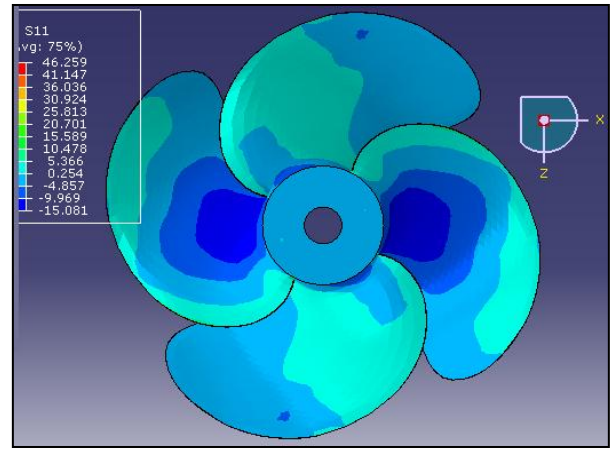


FIGURE: 25 STRESSES IN X-DIRECTION

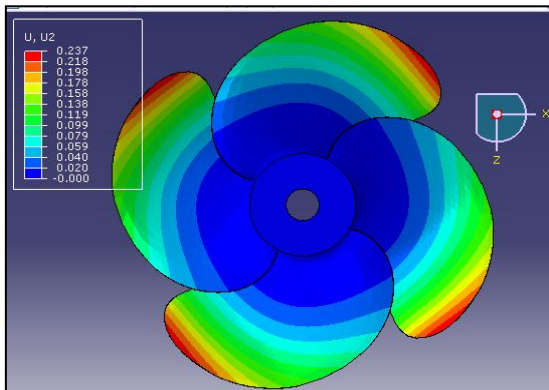


FIGURE: 22 DISPLACEMENT IN Y-DIRECTION

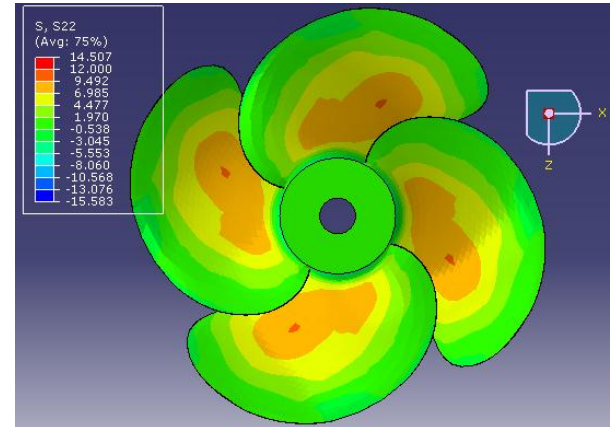


FIGURE: 26 STRESSES IN Y-DIRECTION

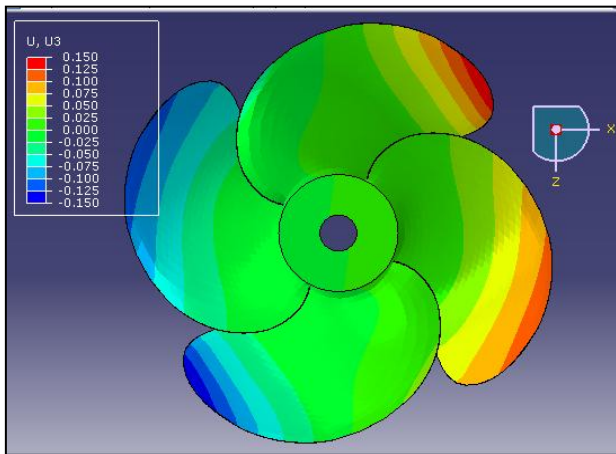


FIGURE: 23 DISPLACEMENT IN Z- DIRECTION

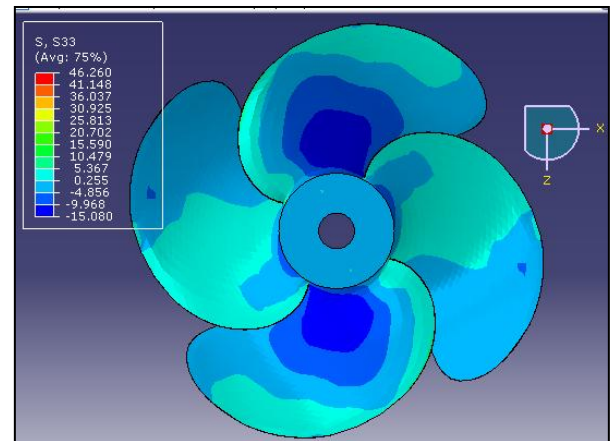


FIGURE: 27 STRESSES IN Z-DIRECTION

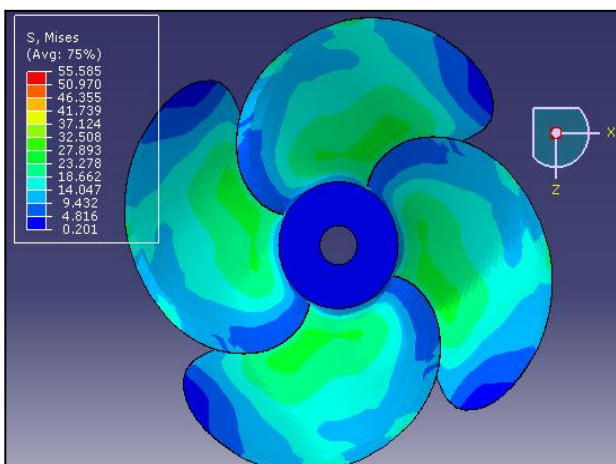


FIGURE: 24 VON MISES STRESS

TABLE: 2  
RESULTS OF ALUMINUM AND COMPOSITE MATERIALS

Element type	Displacement			Stresses(N/mm <sup>2</sup> )			Von misses stresses
	X	Y	Z	X	Y	Z	
Aluminum propeller	0.496	0.396	0.250	77.098	24.179	77.100	92.642
Carbon UD epoxy propeller	0.297	0.237	0.150	46.259	14.507	46.260	55.85

Composite material gives less deformation when the loads are applied. Therefore Composite material propeller is considered for the fatigue analysis of surface piercing propeller.



### C. FATIGUE ANALYSIS OF SURFACE PIERCING PROPELLER:

When propellers are subjected to time varying loads, their behavior is unconditional and it requires a specific methodology to determine them. For example, a particular fiber on the surface of rotating propeller subjected to the action of pressure loads undergoes both tension and compression for each revolution of the shaft, is stressed in tension and compression  $N$  times each minute if the propeller is rotated at  $N$  rev/min.

Machine members are found to have failed under the action of repeated or fluctuating stresses, yet the most careful analysis reveals that the actual maximum stresses were well below the ultimate strength of the material, and quite frequently even below the yield strength. A fatigue failure has an appearance similar to a brittle fracture, as the fracture surfaces are flat and perpendicular to the stress axis with the absence of necking.

The fracture features of a fatigue failure, however, are quite different from a static brittle fracture arising from three stages of development. Fatigue failure is due to crack formation and propagation. A fatigue crack will typically initiate at a discontinuity in the material where the cyclic stress is a maximum.

Discontinuities can arise because of:

- Design of rapid changes in cross section, keyways, holes, etc.
- Elements that roll and/or slide against each other (bearings, gears, cams, etc.) under high contact pressure, developing concentrated subsurface contact pressure that can cause surface pitting (hole) or spalling after many cycles of the load.
- Carelessness (lack of care) in locations of stamp marks, tool marks, scratches, and burrs; poor joint design; improper assembly; and other fabrication faults.
- Composition of the material itself as processed by rolling, forging, casting, extrusion, drawing, heat treatment, etc.

### D. FATIGUE LIFE METHODS:

There are three major fatigue life methods used in design and analysis:

#### 1- Stress-Life Method

- It is based on stress levels.
- The least accurate approach, but most used method, since it is the easiest implement for a wide range of design applications.

#### 2- Strain-Life Method

- Involves more detailed analysis of the plastic deformation at localized regions where the stresses and strains are considered for life estimates.

#### 3- Linear-Elastic Fracture Mechanics Method

- It assumes a crack is already present and detected.
- It is then employed to predict crack growth with respect to stress intensity.
- It is most practical when applied to large structures in conjunction with computer codes and a periodic inspection program.

In this study first method is used, i.e., Stress-Life Method.

### E. FATIGUE LIFE METHODS:

To determine the strength of materials under the action of fatigue loads, four types of tests are performed: tension, torsion, bending, and combinations of these. In each test, specimens are subjected to repeated forces at specified

magnitudes while the cycles or stress reversals to rupture are counted. For the rotating-beam test, a constant bending load is applied, and the number of revolutions (stress reversals) of the beam required for failure is recorded. The first test is made at a stress that is somewhat under the ultimate strength of the material. The second test is made at a stress that is less than that used in the first.

### F. CHARACTERIZING FLUCTUATING STRESSES:

Fluctuating stresses in machinery often take the form of a sinusoidal pattern because of the nature of some rotating machinery. It has been found that in periodic patterns exhibiting a single maximum and a single minimum of force, the shape of the wave is not important, but the peaks on both the high side (max.) and low side (min.) are important. Thus,  $F_{max}$  and  $F_{min}$  in a cycle of force can be used to characterize the force pattern.

$$F_m = \left| \frac{F_{max} + F_{min}}{2} \right|, \quad F_a = \left| \frac{F_{max} - F_{min}}{2} \right|$$

where

$F_m$ : midrange component of force

$F_a$ : amplitude component of force

Many time in design the stresses fluctuate without passing through zero. The following relationships and definitions are used when discussing mean and alternating stresses:

$\sigma_{min}$  = minimum stress

$\sigma_{max}$  = maximum stress

$\sigma_r$  = stress range

$\sigma_s$  = steady or static stress

$$\sigma_a = \text{amplitude stress} = \frac{\sigma_{max} - \sigma_{min}}{2}$$

$$\begin{aligned} \sigma_m &= \text{midrange or mean stress} \\ &= \frac{\sigma_{max} + \sigma_{min}}{2} \end{aligned}$$

$$R = \text{stress ratio} = \frac{\sigma_{min}}{\sigma_{max}}$$

$$A = \text{amplitude ratio} = \frac{\sigma_a}{\sigma_m}$$

#### 8.4.4 Fatigue Failure Criteria for fluctuating Stress:

Varying both the midrange stress and the stress amplitude, or alternating component, will give some formation about the fatigue resistance of parts when subjected to such situations.

Modified Goodman Diagram:

- $\sigma_m$  plotted along the x-axis.
- All other components of stress plotted on the y-axis.
- The modified Goodman diagram consists of the lines constructed to  $S_e$  (or  $S_p$ ) above or below the origin.

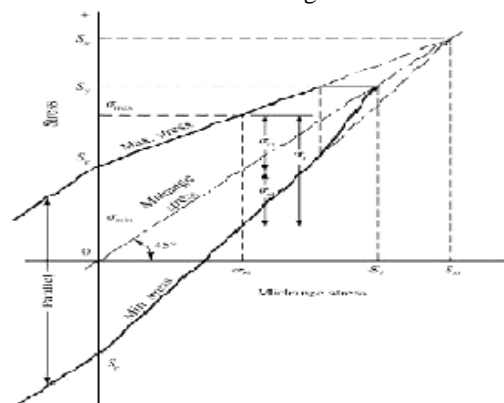


FIGURE 28 MODIFIED GOODMAN'S DIAGRAM

- $S_y$  is plotted on both axes, because  $S_y$  would be the criterion of failure if  $\sigma_{max}$  exceeded  $S_y$ .
- Useful for analysis when all dimension of the part are known and the stress components can be easily calculated. But it is difficult to use for design when the dimension are unknown.
- Modified Goodman's Equation is given by:

$$\frac{1}{n} = \frac{\sigma_e}{S_e} + \frac{\sigma_m}{S_{ut}}$$

The following results are obtained by conducting fatigue test on propeller model. Von -mises stresses, displacement contours are plotted by conducting the test. The results plotted are used to determine the factor of safety.

Figure 8.17 shows displacement contour for carbon UD/Epoxy material.

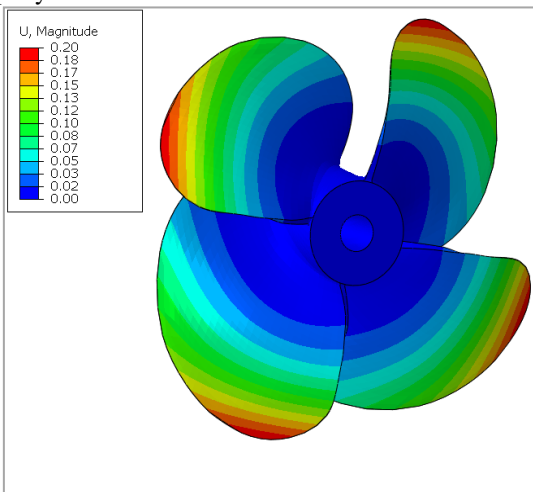


FIGURE: 29 DISPLACEMENT CONTOUR VECTOR SUM

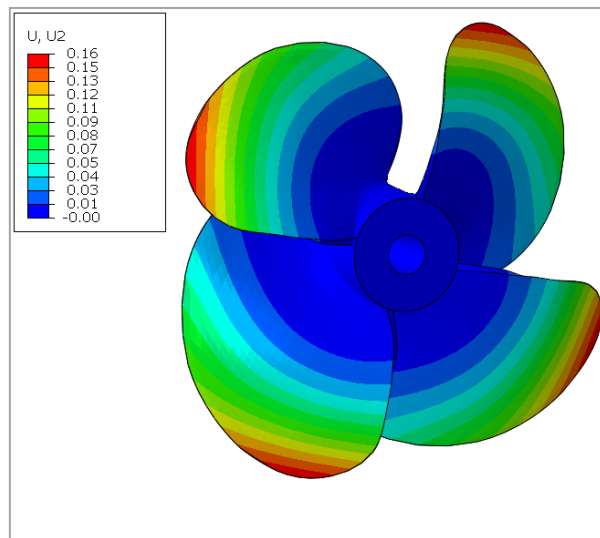


FIGURE: 31 DISPLACEMENT CONTOUR Y- DIRECTION

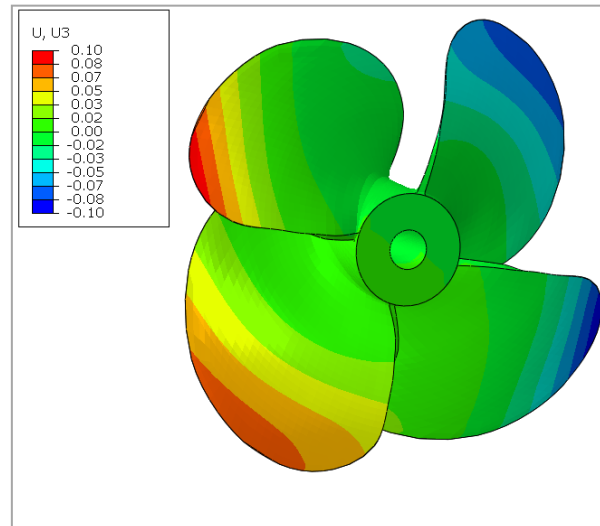


FIGURE: 32 DISPLACEMENT CONTOUR Z- DIRECTION

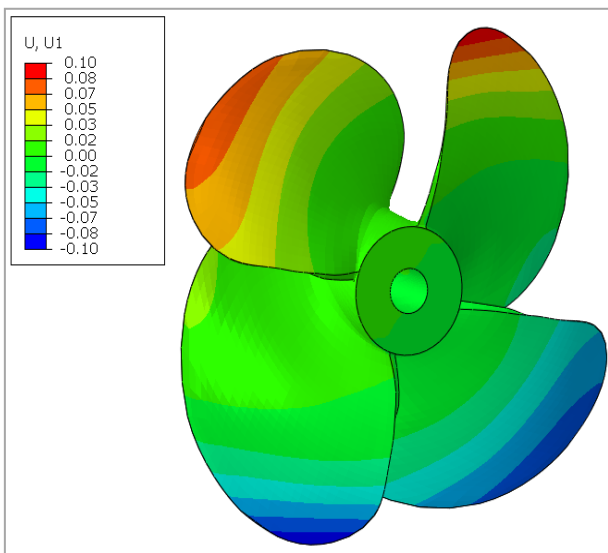


FIGURE: 30 DISPLACEMENT CONTOUR X- DIRECTION

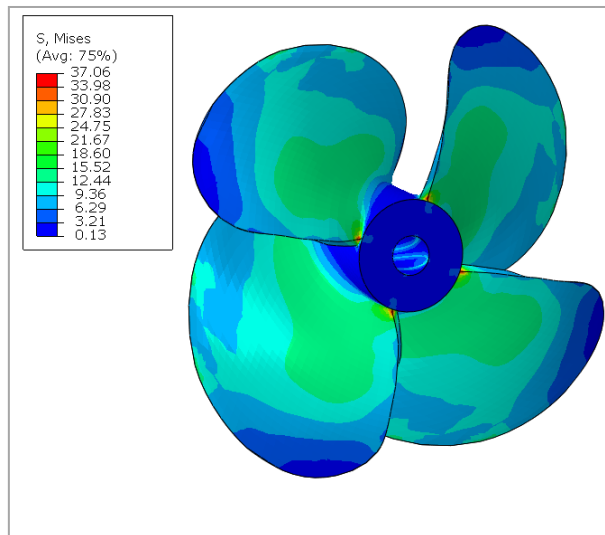


FIGURE:33 VON MISES STRESSES

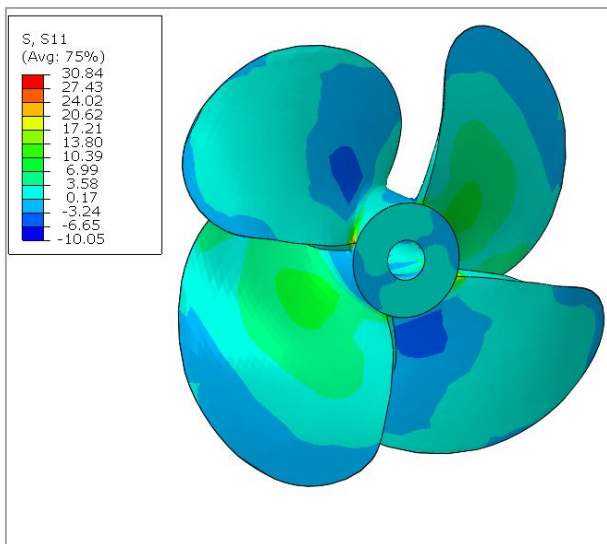


FIGURE: 34 STRESSES X – DIRECTION

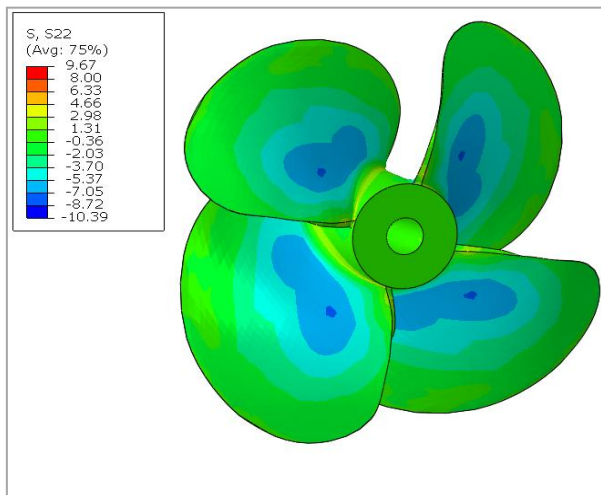


FIGURE: 35 STRESSES Z– DIRECTION

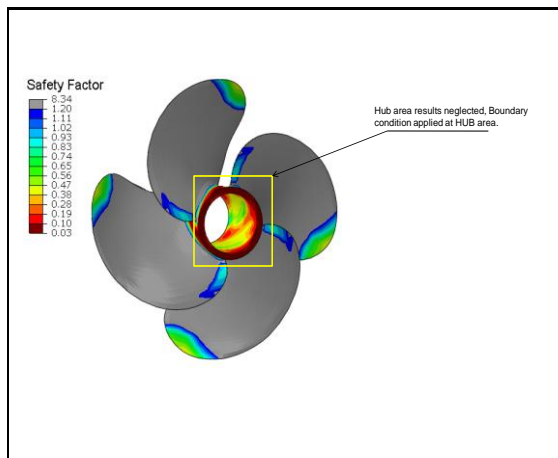


FIGURE: 36 FATIGUE ANALYSIS RESULTS

## VII. CONCLUSIONS

The finite element analysis (FEA) is carried out for two different types of materials, those are aluminum and carbon UD/Epoxy.

Following are the important conclusions drawn from FEA:

- The von-mises stress acting on the propeller produced from aluminum is 92.642 N/mm<sup>2</sup>, corresponding deformation is 0.496mm.
- The von-mises stress acting on the propeller produced from carbon UD/epoxy is 55.585 N/mm<sup>2</sup> and is observed that the value is within the allowable stress

limit. Deformation produced for carbon UD/epoxy material is 0.297mm.

- Fatigue analysis is conducted on the propeller model and the results shows that carbon UD/epoxy material is having good fatigue life with a value of  $1 \times 10^7$  cycles with 0.7 safety factor.
- Finally it is concluded that carbon UD/epoxy material can give a better performance with respect to static analysis and the same material is showing a very high fatigue life.

## VIII. REFERENCES

- [1] J.F.Tsai, H.J.La., Analysis of Underwater Free Vibrations of a Composite Propeller Blade. Journal of REINFORCED PLASTICS AND COMPOSITES, 2008. Vol. 27, No. 5: p. 447-458.
- [2] H.J.Lin, W.M.L.a.Y.M.K., effect of stacking sequence on nonlinear hydro elastic behavior composite propeller Journal of Mechanics, 2010. Vol. 26, No. 3: p. 293-298.
- [3] Toshio Yamatogi, H.M., Kiyoshi Uzawa, Kazuro Kageya, Study on Cavitation Erosion of Composite Materials for Marine Propeller. 2010.
- [4] Young, Y.L., Fluid-structure interaction analysis of flexible composite marine propellers. Journal of Fluids and Structures, 2008 24(6): p.799-818.
- [5] Taylor, D.W., "The speed and power of ships", Washington, 1933.
- [6] J.E.Conolly, "Strength of Propellers", reads in London at a meeting of the royal institution of naval architects on dec 1, 1960, pp 139-160.
- [7] Chang-sup lee, yong-jik kim, gun-do kim and in-sik nho. "Case Study on the Structural Failure of Marine Propeller Blades" Aeronautical Journal, Jan 1972, pp87-98.
- [8] G.H.M.Beek, visitor, Lips B.V., Drunen. "Hub-Blade Interaction In Propeller Strength", the society of naval architects and marine engineers, May 24-25, 1978, pp 19-19-14.
- [9] W.J.Colclough and J.G.Russel. "The Development of a Composite Propeller Blade with a CFRP Spar" Aeronautical Journal, Jan 1972, pp53-57.
- [10] Gau-Feng Lin "Three Dimensional Stress Analysis of a Fiber Reinforced Composite Thruster Blade", the society of naval architects and marine engineers, 1991. J.P Ghosh and R.P Gokaran. "Basic ship propulsion", 2004.
- [11] Paul Kaman, N.A, "Surface piercing propellers", Published in Professional Boat Builder magazine.
- [12] Ch. Suryanarayana, "Manufacture of propellers", Marine propulsion technology, Vol. 1, MPT 1999, pp CSNI-CSNI30.
- [13] Prof.L.C.Burill., "On Propeller Manufacture", The Royal Institute of Naval Architects (RINA), Vol.96, 1954, pp 132-146.

- [14] Yodong Li and PeihuaGu, “Free form surface inspection techniques state-of-the-art review”, Computer aided design, Vol.36, November 2004,pp 1395 -1417.
- [15] Mark.F.Nittel, “Numerical Controlled Machining of Propeller Blades”, Marine Technology, Vol. 26, No.3, July 1989, pp 202-209.
- [16]J.P. Ghose& R.P. Gokarn, “Basic ship propulsion,” Allied publishers, 2004. J.S. Carlton, “Marine Propellers and Propulsion”, Butterworth-Heinenann Ltd 1994, Oxford 1994.
- [17]“Marine Engineering” by a group of authorities, published by The Society of Naval Architects and Marine Engineers.